

Using Spatial Context in Satellite Data to Infer Regional Scale Evapotranspiration

JOHN C. PRICE

Abstract—Several methods have been used to estimate regional scale evapotranspiration from satellite thermal infrared measurements. These procedures assume knowledge of surface properties such as surface roughness, albedo, vegetation characteristics, etc. In many areas of the earth these parameters are not accurately known due to the rapidity of change of vegetation, lack of adequate geographical data bases, and the low spatial resolution of satellite data which results in multiple surface types corresponding to each satellite measurement. In this paper, an estimate of evapotranspiration is developed by relating variations of satellite-derived surface temperature to a vegetation index computed from satellite visible and near infrared data. The method requires independent estimates of evapotranspiration for a completely vegetated area and for a nonvegetated area, although such areas need not appear in the satellite data. A regional estimate of evapotranspiration is derived despite the lack of precise estimates for individual satellite measurements. The method requires spatial variability in the satellite data: it does not apply in uniform areas. In addition, a property is identified which permits discrimination of cirrus clouds from areas of varying soil moisture. A data bank of surface characteristics should be developed to support description of surface processes at large scales.

I. INTRODUCTION

DURING the last 10 years substantial progress has occurred in the use of satellite data to estimate evapotranspiration over large areas. Improved numerical models [3], [4], [23], [24] and field experimentation have led to procedures of reasonable accuracy and generality for the description of moist surfaces of varying types. These methods may be applied, at least in principle, to satellite observations over the entire earth, yielding data required for input to general circulation models as well as for improved descriptions of the earth's atmosphere at the mesoscale [22]. Although the land surface is quite nonuniform at the 50–200-km scale of description used in forecast models, a procedure developed for aggregating results derived from subareas in a heterogeneous region can produce parameterized values appropriate for input to such models [13]. Thus the problem might appear to be solved.

At present, methods of analysis assume that values are known for surface roughness, albedo, and emissivity, plus canopy parameters for vegetated areas. This assumption applies to small experimental data sets for case studies, where reasonable estimates or measurements are feasible.

However, the assumption is unsatisfactory for many regions, where detailed knowledge is either unavailable, or else the surface is too variable in time and space for the information to be commonly available. This applies for many temperate regions which receive moderate rainfall, i.e., the regions of human habitation. In these areas surface conditions continually change according to agricultural practices, industrial uses, clearing and burning, reforestation, etc. Furthermore, the appropriate sensor for global studies, the advanced very high resolution radiometer (AVHRR) which acquires 1.1-km data at nadir, lacks adequate spatial resolution to resolve most fields, especially when the larger picture elements from off nadir viewing are considered. In principle this is not a problem, if detailed information regarding surface properties within each measured area is available. Existing analysis methods for thermal infrared data describe the surface energy and moisture fluxes, given local ground parameters [4], [14], [30]. Thus analysis at small scales followed by aggregation of results from each field or surface type would appear to provide a solution.

In fact, this procedure is not generally applicable, as even the high spatial resolution satellites, Landsat and SPOT, do not provide adequate coverage frequency to monitor vegetation changes, and hence, evapotranspiration, in view of the likelihood of cloud cover. Also such an approach would be prohibitively expensive.

Figs. 1 and 2 illustrate the problem. These Landsat images, representing surface temperature and vegetation index, show that variability in agricultural areas is commonly at a scale of 100's of meters, rather than the 1-km scale of AVHRR data. However, Landsat overpasses occur only at 16-day intervals. Considering cloud cover, the interval between observations becomes on the order of 1–2 mo, which is inadequate for the desired purpose. In addition the mid-morning timing of Landsat observations is less than optimum for estimating moisture conditions from the thermal infrared data [16], while SPOT does not carry a thermal IR channel. On the other hand, it is clear that aggregation of Landsat data to the AVHRR scale would result in multiple surface types for each AVHRR data point. While it is possible to sum results for surface energy fluxes over subareas with known properties, the inverse problem, to describe accurately the evapotranspiration within each AVHRR data point without specific knowledge of the associated physical parameters, is generally insoluble. It is this problem which we address, bas-

Manuscript received October 21, 1989; revised January 3, 1990.
The author is with the Agricultural Research Service, United States Department of Agriculture, Beltsville, MD 20705.
IEEE Log Number 9035839.

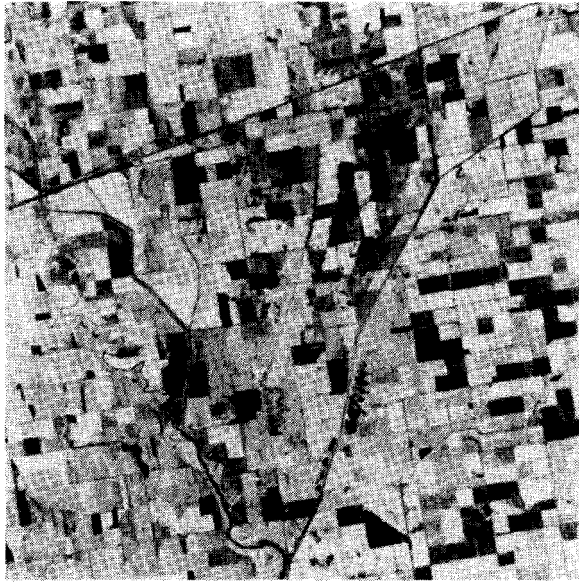


Fig. 1. Vegetation index derived from Landsat thematic mapper data at 28-m spatial resolution, with higher values bright, lower values dark. Most fields are of order 10 hectares in area. This agricultural area corresponds to approximately 170 AVHRR measurements.



Fig. 2. Temperature values corresponding to Fig. 1. The picture is less sharp due to the 120-m resolution of the thematic mapper thermal IR channel. In this paper high radiances (high temperature) are brighter, while darker areas are cooler. These darker areas correspond to vegetation (compare with Fig. 1).

ing a statistical approach on the man-induced and natural variability typical of most areas. The approach illustrates the need for a reference data base or "geobased information system" to support the statistical method.

If we consider the surface of the earth, we may partition it, roughly speaking, into water, snow, and ice, which have known moderately constant properties (except tem-

perature), mountains, deserts, forest, and tundra, which are complex and not well described, but at least are relatively uniform on a spatial scale of 10's of kilometers, and the narrow strips in the temperate latitudes which are dominated by agriculture. Although these latter areas appear to be negligible in the description of global weather and climate, two factors raise their importance significantly: 1) the global supply of food and fiber has social and political implications, making an accurate description desirable, and 2) a major part of the area is subject to considerable rainfall variations, including drought, which can have implications for the surface-atmosphere interaction if these variations are prolonged. Thus mid-latitude rainfall and vegetation conditions are sensitive indicators of climate, as well as affecting the evolution of the earth-atmosphere system through proposed feedback mechanisms [6].

Section II discusses the surface energy and moisture balance, as may be inferred from satellite data. A vegetation index is useful in discriminating vegetation from soils, which have very different moisture transfer characteristics. Section III addresses spatial variability within AVHRR observations and develops a procedure for inferring regional scale properties even though a detailed mapping of surface characteristics at the AVHRR spatial scale is not feasible. The method is applied to a data set in the U.S. Great Plains, illustrating that several types of information may be discriminated in the data, provided the area imaged is nonuniform. The need for a statistical data base of surface properties at low spatial resolution (e.g., 1° grid spacing) is discussed in the conclusion in Section IV.

II. ELEMENTS OF THE SURFACE ENERGY AND MOISTURE BALANCE

The fluxes of energy, momentum, and moisture at the earth's surface are influenced both by meteorological conditions and by the physical state of the surface itself. Some surface variables may be inferred from remote sensing.

A. Surface Temperature and Emitted Radiation

Surface temperature is a major indicator of the partitioning of energy at the earth's surface through its effect on latent and sensible heat flux to the atmosphere, sensible heat flux into the ground, and radiation to the atmosphere and space. Satellite thermal infrared measurements have been used for many years for estimation of global sea surface temperatures. However, the estimation of land surface temperatures extends the range of temperatures well above those of water, and variability of surface emissivity represents an additional complication. In this paper we use the formula of Price [15], which was shown to be consistent with both the empirically derived sea-surface temperature relationship and with radiative transfer theory:

$$T_{BB} = T_4 + 3.3 \cdot (T_4 - T_5). \quad (1)$$

Here T_{BB} is the estimated surface radiance temperature and T_4 and T_5 are the radiance temperatures derived from AVHRR thermal infrared channels at 10.8 and 12.9 μm . Radiance temperature must be adjusted for the effect of surface emissivity. We correct a sign error in Price [15, section 4] with the proper account of emissivity being given by

$$T_s = [T_4 + 3.3 \cdot (T_4 - T_5)] \cdot (5.5 - \epsilon_4) / 4.5 - 0.75 \cdot T_4 \cdot (\epsilon_4 - \epsilon_5) \quad (2)$$

where ϵ_4 and ϵ_5 are the emissivities in the respective spectral bands and T_s is the surface temperature. Since the spectral variation of emissivity is generally unavailable, so we simply take $\epsilon_4 = \epsilon_5 = 0.96$. In any event, accurate quantitative results depend on the calibration of the AVHRR sensor, which is not well established for the range of mid-day land temperatures.

B. Albedo

Surface albedo may be estimated from data in AVHRR channels 1 and 2, representing wavelength ranges 0.58–0.68 and 0.73–1.10 μm . These spectral intervals do not represent the full solar spectrum, and therefore, do not measure the full spectral reflectance values. Also, angular variations occur in the satellite data and must be averaged out or corrected for by means of a theoretical formulation Gutman [8].

C. Vegetation Index

The presence or absence of vegetation causes significant differences in surface energy and moisture fluxes. Vegetation can extract water from significant depths, e.g., 1 m for annual crops and 10 m for trees, affecting surface hydrology as well as contributing an atmospheric moisture flux over periods of days or weeks. In contrast, bare soil is usually, to a first approximation, either wet or dry: fluxes from beneath the first few centimeters are generally very small. Vegetation also increases surface roughness, to a slight extent for agricultural crops, to a much larger degree when trees, scattered bushes, and brush are present. In contrast, bare soil rapidly erodes to a very smooth condition.

Atmospheric models do not predict the presence or absence of vegetation: this is a boundary condition. This input can be a demanding task in areas of significant variability. Fortunately, satellite reflectance measurements in the visible and near infrared can yield part of this information in a timely fashion. However, there is no standardized formula for deriving the degree of vegetation cover from the satellite data. From a number of formulas which have been proposed we select the normalized difference vegetation index (NDVI) [7], [10], [12], [17], [31]:

$$\text{NDVI} = \frac{(a_2 - a_1)}{(a_2 + a_1)} \quad (3)$$

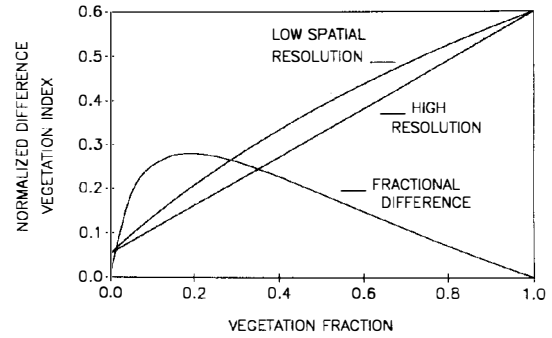


Fig. 3. The normalized vegetation index does not satisfy the associative property, as illustrated by the difference between hypothetical high resolution measurements and low resolution (average) values. For computation purposes $a_{1v} = 0.12$, $a_{2v} = 0.48$, $a_{1g} = 0.18$, and $a_{2g} = 0.20$. The relative difference approaches 30%.

where a_1 and a_2 are the reflectance values measured by channels 1 and 2 of the AVHRR. In AVHRR data NDVI values generally vary from low values of 0.0–0.05, based on equality of the visible and near IR reflectances, to values of approximately 0.65 at the upper limit [26], [27]. It must be emphasized that NDVI is simply an index, and does not have a unique correlation with vegetation cover.

NDVI has the undesirable property that the value computed does not satisfy the associative property for area measurements, being affected by the spatial resolution of the measuring instrument. Thus in general,

$$A \cdot \text{NDVI}(A) + B \cdot \text{NDVI}(B) \neq (A + B) \cdot \text{NDVI}(A + B) \quad (4)$$

where A and B are contiguous areas. The discrepancy occurs when the spatial inhomogeneity of the area is large. This follows from the fact that NDVI is a ratio. Thus

$$f \cdot \frac{(a_{2v} - a_{1v})}{(a_{2v} + a_{1v})} + (1 - f) \cdot \frac{(a_{2g} - a_{1g})}{(a_{2g} + a_{1g})} \neq \frac{[f \cdot (a_{2v} - a_{1v}) + (1 - f) \cdot (a_{2g} - a_{1g})]}{[f \cdot (a_{2v} + a_{1v}) + (1 - f) \cdot (a_{2g} + a_{1g})]} \quad (5)$$

For example, Fig. 3 illustrates the values obtained for a region consisting of a mixture of totally vegetated area (v) with fractional area f , and nonvegetated (g) area with fraction $1-f$, where we have assumed that the different surfaces are completely resolved by the sensor. Evidently the proper straight line relationship between NDVI and fractional vegetation cover is not reproduced by a hypothetical sensor which acquires with a single measurement the vegetation index of an area of mixed cover. The fractional difference can approach 30% for intermediate mixtures of vegetated and nonvegetated surfaces. Evidently, additional information is required to distinguish between a uniform vegetation cover of relatively low density, as with a crop in early growth, or a drought distressed area, versus an area with healthy soil hiding vegetation alternating with bare or fallow areas. Both could have the same total

vegetation cover, while yielding different values of vegetation index. A somewhat different aspect of this problem, the association of inhomogeneity within forests with moisture variations, has been considered by Nemani and Running [20]. Figs. 1 and 2 and satellite imagery in Section III illustrate the significance of vegetation as a factor of the surface energy and moisture budget.

III. INFERENCE OF REGIONAL EVAPOTRANSPIRATION FROM HETEROGENEOUS AREAS

Because of the complexity of the interaction of the earth's surface and atmosphere, we limit ourselves to developing a method estimating the moisture flux. The problem of interpreting AVHRR data has two aspects, one being the availability of surface parameters, the other the method of analysis, given these data. First, a quantitative description of vegetation and soil characteristics is not generally available at regional scales. Thus one could not go to a general location and account properly for the evolution of surface fluxes, even with the benefit of first hand information on the presence and status of vegetation and the capability to disturb the soil. Instead, one would have to rely on typical values from the literature, if available, for surface roughness, soil moisture retention characteristics, etc., or else establish such data by research. Generally, satellite data may augment typical atlases giving a general climatic/ecological description. Unfortunately, neither conventional studies nor satellite based work to date emphasizes the development of values for surface roughness, canopy structure, moisture processing efficiency, etc., as are required for atmospheric modeling. These data for regional assessment could also be acquired by analysis of a sampling of statistically based ground sites.

Secondly, even given the basic properties of land cover in a region, we do not know the fraction of different surface types within the large (120 hectare) areas of each AVHRR measurement. The reason for diverse vegetation cover in mid-latitudes is largely economic: in order to reduce economic risk, farm units select a number of vegetation (crop) types. The mix and rotation of selected varieties tends to prevent depletion of soil fertility, so that a time invariant description of each land unit is not possible. In other areas activities such as forest clearing, irrigation projects, and changing population density produce local nonuniformity of the earth's surface. To the degree that high resolution satellites can discriminate different land covers, this problem is straightforward in principle. Unfortunately, it is currently intractable and may remain so indefinitely. However, if such a comprehensive description is not required and regional values are satisfactory, then the procedure developed here appears acceptable. This does not obviate the need for quantitative parameters for representative surface types. Furthermore, the accuracy of the statistical description developed here should be established based on examination of complete data sets. For this purpose, a study of carefully documented experimental data is needed [5].

A. Procedure

We must allow for variability of the surface conditions and a mixture of surface types within each area corresponding to a satellite measurement. We consider each area to be comprised of a mixture of a vegetated area and an area of bare soil and/or dead vegetation. The properties of the individual components may not be accessible in the data, and the suitability of the analysis must be verified from the data itself. We shall compute the values obtained from the "mixed pixels" or heterogeneous measurement areas, using the notation of Section II. Thus for measurements with mixed surface types, the satellite measured radiance is given by $\Sigma a = a_v + a_g$ and we write the normalized difference vegetation index at a point p in the form (henceforth, we abbreviate NDVI to V):

$$V_p = f \cdot V_v + (1 - f) \cdot V_g \quad (6)$$

where V_p is the remotely obtained value of the vegetation index. From Fig. 3 we see that the satellite data tend to overestimate the vegetation index for an inhomogeneous area as compared to a uniform vegetation density. This effect is marginally noticeable in the data which are discussed later.

In the AVHRR thermal infrared channels 4 and 5 we approximate the satellite measured radiance by $\epsilon\sigma T^n$, with $n\lambda \approx 4.5$ for the 10–12 μm spectral interval. Then we may use (2) to estimate surface temperature, and for a modest temperature range, c.g. 20°–40°C within a resolution element, we write

$$T_p = f \cdot T_v + (1 - f) \cdot T_g \quad (7)$$

where T_p is the apparent temperature, representing a weighted sum of values from vegetation and soil. On examination of typical data sets one finds a clear tendency for more vegetated areas to be cooler than nonvegetated areas. For such cases, and *provided that the area in question is nonuniform*, we relate V and T_s by forming the ratio, i.e.:

$$R = \frac{f \cdot V_v + (1 - f) \cdot V_g}{f \cdot T_v + (1 - f) \cdot T_g} \quad (8)$$

where the ratio may be obtained from a regression of V on T , or by plotting a two-dimensional scattergram of the data. The correlation coefficient provides a guide as to the applicability of the method. We note that the ratio retains the factor f , indicating that the slope is not precisely constant. In evaluation of real data this is unimportant, as the basic assumptions do not hold exactly. In particular, the breakdown of the associative property discussed earlier implies a difference between a uniform area of constant vegetation density, versus a mixture of bare and fully vegetated fields, as may be expected in data used in this section. Now, given the slope R and intercept of the NDVI/ T_s line, we may evaluate the temperature of total vegetation cover and the temperature of zero vegetation cover, corresponding to evaporating and dry surfaces, respectively. This does not imply that all vegetation types

transpire at the same rate, but that differences in transpiration at full vegetation cover are associated with differing values of NDVI. In the data presented here this represents an extrapolation from a middle range of values. Evidently this extrapolation is not possible if a range of T_s and V values does not exist. From the temperature values extrapolated to full vegetation cover and zero vegetation we derive values for the evapotranspiration of the two surface types from a simulation model [13], [14]. Such models use surface meteorological data plus such assumed parameters as are required for computation of surface temperatures. The appropriate value of evapotranspiration corresponds to that derived from those parameters yielding a surface temperature equal to the satellite derived temperature. The total evapotranspiration for each satellite measurement is the sum of the weighted values from bare soil and vegetation, where the vegetation index provides the key to the relative fractions. Finally, the regional value is obtained by summing over all data points.

B. Application to a Satellite Data Set

The data set discussed here [15] has the desirable property of representing a very large relatively cloud-free area at a time of considerable regional variability in moisture conditions. This was associated with large spatial differences in rainfall in the mid-west U.S. during the summer of 1981. Figs. 4 and 5 illustrate vegetation index and temperature for a portion of southeast Texas on July 20, 1981. Conventional data [29] show that soil moisture conditions were generally adequate closer to the Gulf coast at the lower right, becoming drier inland toward the upper left. The visual association of temperature with vegetation index is confirmed by a two-dimensional scattergram (Fig. 6). We note from the figure that the range of values does not extend from purely bare soil ($V \approx 0.1$) to total vegetation cover ($V \approx 0.6$). However, it is evident that we may extrapolate a linear fit to obtain estimates $T_r = 30^\circ\text{C}$ and $T_g = 64^\circ\text{C}$ for the two cover types. For these data the regression line is given by

$$V = 1.08 - 0.016T(^{\circ}\text{C}), \quad R^2 = 0.81. \quad (9)$$

The correlation between the temperature and vegetation index for such heterogeneous areas provides the basis for the method developed here. We do not derive a value for evapotranspiration for this case because a nearby area requires consideration of surface soil moisture variation as well as vegetation cover.

The second area considered is in the state of Nebraska. At the date of the satellite data acquisition, Nebraska had some areas of adequate soil moisture and other areas of drought. An appreciation for the spatial variability may be gained from Figs. 7 and 8. The regions in the upper left and lower right of the vegetation index image represent irrigated areas along the North Platte river. Comparison of the images shows the expected association of a high temperature, low vegetation index. However, Fig. 8 shows that a substantial portion of the total nonvegetated area is cool (dark) relative to other areas which are also

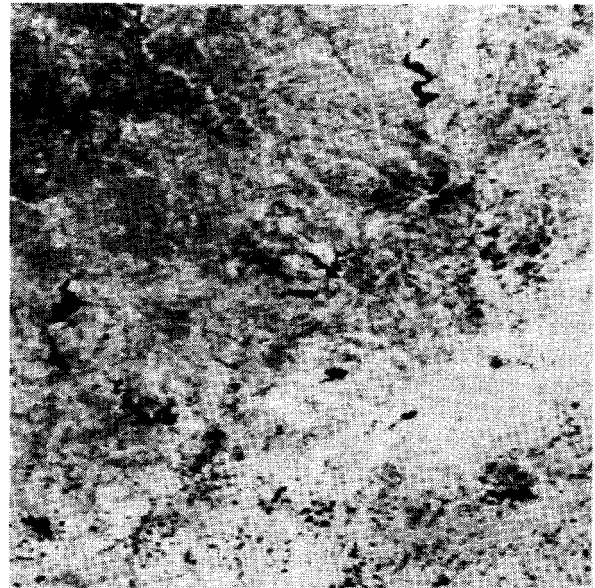


Fig. 4. Vegetation index on July 20, 1981 for an area in east Texas approximately 280 km on a side. The northeast-southwest gradient agrees with the soil moisture index of the NOAA/USDA *Weekly Weather and Crop Bulletin* [29].

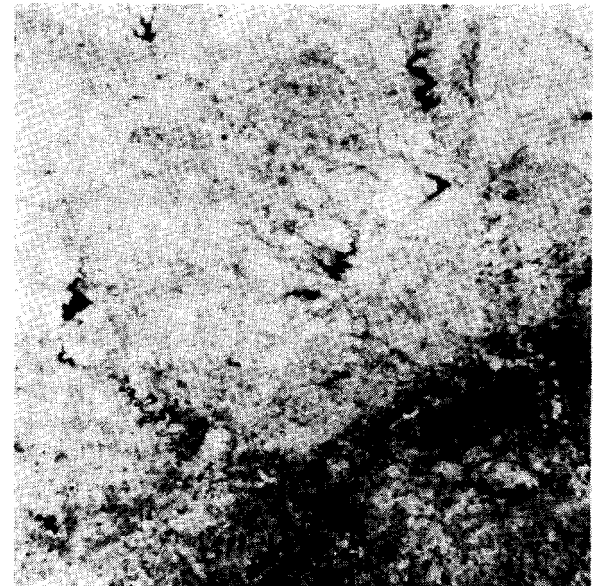


Fig. 5. Surface temperature values corresponding to Fig. 4, as derived from AVHRR channels 4 and 5.

not vegetated. Such diffuse patterns are common in satellite thermal infrared data, being caused by either moist surface conditions or lower apparent temperatures due to cirrus clouds. This latter possibility is discussed later. In this example we associate the cooler pattern with increased surface moisture in the soil and stubble remaining from harvested winter wheat. During the 1981 summer season this area was affected by spotty rainfall, as de-

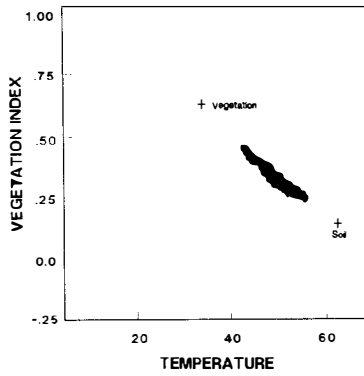


Fig. 6. A scattergram of vegetation index and temperature (°C) corresponding to Figs. 4 and 5. The best fit line is used to extrapolate temperatures for bare soil and complete vegetation cover.



Fig. 7. Vegetation index for an area in western Nebraska on July 20, 1981. The bright area at the right center is an irrigated region along the North Platte river.

scribed in the Weekly Weather and Crop Bulletin [29]. However, a detailed comparison with maps given there is not feasible due to the low density of the rainfall observation network. The scattergram of observations as a function of T and V is presented in Fig. 9. From the figure we identify several associations. First, the upper edge of the population shows the expected relationship, corresponding to Fig. 6, between temperature and vegetation cover. However, the range of values is considerably larger than in Fig. 6, illustrating the presence of irrigated agriculture along the North Platte river, in the midst of an area which is generally hotter and drier than Texas at this season. Secondly, a considerable temperature range exists for low values of vegetation index. Examination shows that this range corresponds to the dark-to-bright variation in the nonvegetated areas in Fig. 8; i.e., to a range of soil

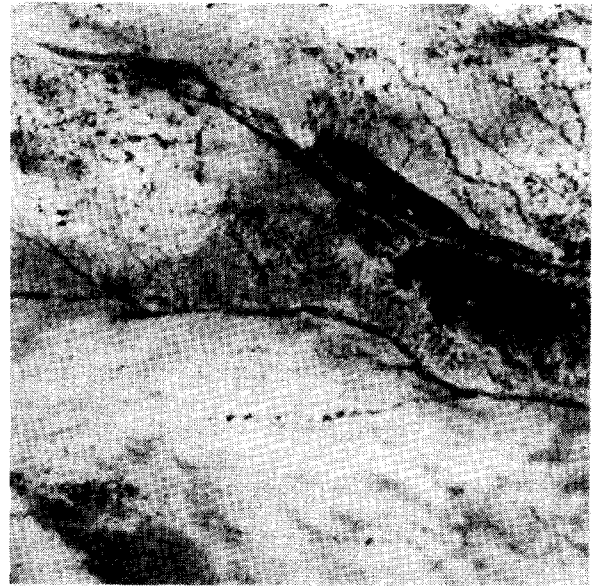


Fig. 8. Surface temperatures corresponding to Fig. 7. The blotchy areas are cooler due to soil moisture associated with recent rainfall.

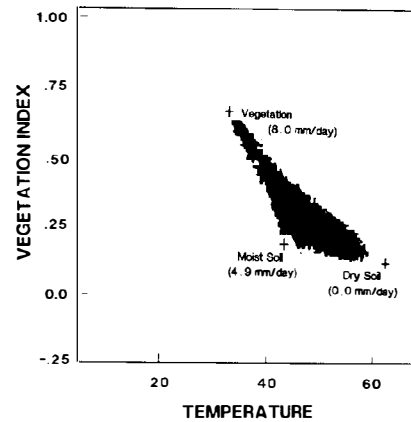


Fig. 9. A scattergram of V versus T_s (°C) from Figs. 7 and 8. The spreading of the temperature values at low vegetation index is due to varying degrees of surface moisture, in general agreement with patterns of moisture in the Weekly Weather and Crop Bulletin [29]. The locations of points corresponding to total vegetation cover, dry soil, and moist soil are derived from the borders of the population of observations.

moisture. Thirdly, higher values of vegetation index occur in areas of both wet and dry soils. Thus the scattergram in Fig. 9 corresponds to varying mixtures of vegetation, dry soil, and wet soil, the latter having low values of vegetation index. We assume that soil of intermediate moisture may be treated as a weighted sum of wet and dry soil, where the borders of the scattergram, extended if necessary, define the locations of wet and dry soil and vegetation. Then letting subscript 1 correspond to vegetation, 2 to dry soil, and 3 to wet soil, we have

$$\begin{aligned}
 T_p &= f_1 T_1 + f_2 T_2 + f_3 T_3 \\
 V_p &= f_1 V_1 + f_2 V_2 + f_3 V_3
 \end{aligned}
 \tag{10}$$

where $f_1 + f_2 + f_3 = 1$. The solution for a fraction f_i may be verified by inspection:

$$f_i = \frac{T_p \cdot (V_j - V_k) + V_p \cdot (T_k - T_j) + T_j V_k - T_k V_j}{T_i \cdot (V_j - V_k) + V_i \cdot (T_k - T_j) + T_j V_k - T_k V_j}, \quad (11)$$

$$i, j \neq k = 1, 2, 3.$$

The moisture flux at a location with temperature and vegetation index values T_p, V_p , is given by

$$\text{LE}(T_p, V_p) = f_1 \cdot \text{LE}(\text{dry soil}) + f_2 \cdot \text{LE}(\text{moist soil}) + f_3 \cdot \text{LE}(\text{vegetation}) \quad (12)$$

where the LE values on the right are from a numerical simulation which predicts observed temperature as a function of surface parameters, including albedo, moisture availability, etc., plus necessary meteorological data, such as surface wind, air temperature, and humidity. Surface weather observations from the North Platte were used in the computations. Table I provides the values assumed, measured from the satellite data (Fig. 9), or resulting from calculation, for the essential physical parameters. These parameters are the moisture availability, which is the ratio of evaporation rate to potential evaporation, and the diurnal heat capacity $= (\Omega \rho c \lambda)^{1/2}$, a heat storing resistance related to Ω , the earth's rotation rate, and ρ, c , and λ , which are, respectively, the effective density, heat capacity, and thermal conductivity for soil or soil and vegetation, plus quantities discussed earlier. Values for moisture availability and diurnal heat capacity have been selected to produce temperature values for the points indicated in Fig. 9. The assumed values are reasonable but essentially arbitrary in the absence of specific information about the region. The values for V and surface temperature were obtained by analysis of the scattergram of Fig. 9. Evidently a data base of regional properties is needed.

It is desirable to normalize the two-dimensional probability of observations at values T, V ; i.e., we normalize the probability density:

$$\iint dT dV P(T, V) = 1. \quad (13)$$

Then the total evapotranspiration over the area is given as a summation, which may be expressed in the space of surface temperature T_s , and vegetation index V ; i.e.:

$$\text{LE} = \iint dT_s dV \text{LE}(T_s, V) P(T_s, V). \quad (14)$$

Because $\text{LE}(T_s, V)$ is a weighted sum of known values (12), it is possible to relate the final result to averages of the distribution P . Thus

$$\langle \text{LE} \rangle = \sum_{i \neq j \neq k} \text{LE}_i \cdot [\langle T \rangle \cdot (V_j - V_k) - \langle V \rangle \cdot (T_j - T_k) + (T_j V_k - T_k V_j)] / N \quad (15)$$

where $N = \sum_{i \neq j \neq k} [T_i \cdot (V_j - V_k)]$, i, j , and k are represented in cyclic order, and the brackets $\langle \rangle$ represent area averages. Since these average values correspond to a

TABLE I
PHYSICAL PARAMETERS DESCRIBING VEGETATION, DRY SOIL, AND WET SOIL FOR AN AREA IN NEBRASKA

Parameter (unit)	Vegetation	Moist Soil	Dry Soil
Surface roughness ^a (m)	.05	.0005	.0005
Diurnal heat capacity ^a ($\text{W} \cdot \text{m}^{-2} \cdot \text{C}^{-1}$)	3.	13.	5.
Albedo ^a	.20	.10	.15
Surface Temperature ^m (C)	33.	43.	62.
Vegetation index ^m	.65	.18	.14
Moisture availability	.80 ^c	.50 ^c	0.0 ^a
Evapotranspiration ^c (mm/day)	8.0	4.9	0.0

a assumed
m measured
c computed

simple area average it is appropriate to ask what has been gained through use of the T/V diagram. In fact the utility of this approach results from the capability to estimate the locations (T_i, V_i) of the respective values for pure vegetation cover, for dry soil, and for moist soil. These locations permit estimation of the respective LE_i values, which in turn permit estimation of LE values for areas of mixed surface types through (11)–(15). For the area in Nebraska the resultant value for area average evapotranspiration is $\langle E \rangle = 5.3 \text{ mm H}_2\text{O/d}$.

Finally, it should be noted that a number of small water bodies are apparent in both the Texas and Nebraska areas, as well as scattered cumulus clouds. These have been ignored in the calculations, although they could be excluded by simple image processing methods. While clouds should be eliminated as unrepresentative of surface conditions, the water bodies in effect provide additional context through their temperature and reflectance values. Such information could, in principle, be used to augment correction of satellite data for atmospheric effects, as well as to refine the estimate of evaporation. However, the values assumed in Table I should be derived from known parameterization of the surface characteristics. In addition many of the simplifications of this paper, including the details of the simulation model, should be dealt with for a more accurate description of surface processes.

C. Error Sources

There exist three independent sources of error in the present study. The first is associated with the sensitivity of the surface temperature to values of surface parameters, to meteorological conditions, and to the simulation model. Such effects have been considered in early literature in the field [2], [21]. Generally, there is no advantage to using a sophisticated simulation model if the surface parameters required as input data are not available for the region in question. A second error source is associated with the analysis of satellite data. Atmospheric variability affects radiances in the visible and near infrared [9], since the effect of aerosols cannot generally be established readily in the satellite data. The calibration of the data is not

well established [1], [25] and prelaunch values of radiance calibration coefficients have been published only recently [17]–[19]. In addition the description of bidirectional reflectance effects is still empirical, so that the angular variations associated with AVHRR observations may be considered a source of error [7], [8]. Error sources for the thermal infrared data have been discussed by Price [15]. Thirdly, the analysis in this paper introduces error through the estimation of the location of the points representing total vegetation, dry soil, and moist soil. In Fig. 9, these points may reasonably be inferred from the scattergram, so that the issue of viewing effects and calibration of AVHRR channels 1 and 2 is unimportant. More frequently the scattergram represents vegetation and dry soil, as illustrated in Fig. 6. In this case errors are associated with viewing effects and with the selection of region specific numerical values for vegetation index of full vegetation cover and bare soil. In addition, the selection of representative values of physical parameters for the energy balance computations is an error source until a formal procedure is given for specifying them on a regional basis.

D. Discrimination of Moist Soil from Cirrus Clouds

Those familiar with satellite thermal infrared data will recognize that the darker blotchy areas in Fig. 8 resemble contamination of the thermal infrared data by cirrus cloud cover. Thin cold cirrus clouds are frequently essentially invisible, or “subvisible” in the visible spectral range, while lowering temperatures noticeably in the thermal infrared. In the above example we may eliminate this possibility based on examination of contextual information. If cirrus clouds exist then their radiating temperature is much lower than any surface features: typically in the range 200–240 K. Thin cloud cover will have the effect of lowering temperatures of all surface features, including vegetation. Thus we should expect to see a difference in temperature between vegetation in the proposed cirrus areas, versus that in uncontaminated areas. This test is easily applied to the Nebraska data set, yielding the unambiguous conclusion that vegetation temperatures are the same in both areas. Thus the blotchy appearance is indeed due to surface moisture variations rather than to cirrus contamination. We note that once again this discrimination requires nonuniformity in the data set.

IV. CONCLUSION AND RECOMMENDATIONS

A method has been developed for relating contextual information (the slope of the vegetation index—surface temperature line and the slope of the wet soil—dry soil line) in AVHRR data to large area evapotranspiration. This procedure permits estimation of latent heat flux in regions where high spatial variability prevents use of more sophisticated methods requiring detailed knowledge of surface characteristics. Instead, only appropriate regional values of vegetation and soil characteristics are required. Application of this method for weather and climate purposes requires knowledge of appropriate roughness, veg-

etation canopy structure, albedo, etc., on a global basis. Such data are not generally available, although a description of global land surfaces has been developed [11] based on examination of satellite data. However, the description presented there is taxonomic; i.e., naming rather than quantitative. Evidently it would be desirable to establish appropriate parameters affecting the surface energy balance, e.g., albedo, surface roughness, moisture release characteristics such as stomatal resistance, rooting depth, seasonal variability, etc., as functions of the vegetation type. In areas of conventional agriculture it would be desirable to have as well a rudimentary knowledge of cropping practices, because the weakness of the normalized difference vegetation index with respect to submeasurement variability is most significant in these areas where crop/fallow distinctions can mimic poor growth of a uniform vegetation stand. In such areas either ground information is required to support statistical use of the AVHRR data, or else data from the high resolution sensors (Landsat, SPOT) must be used to characterize the surface at the scale finer than the 1.1-km spatial resolution of the AVHRR. An atlas or data base for regional surface characteristics is necessary for further progress in the global description of processes at the earth’s surface.

ACKNOWLEDGMENT

The author is indebted to S. Running for suggestions which have improved the manuscript.

REFERENCES

- [1] P. Abel, G. R. Smith, R. H. Levin, and H. Jacobowitz, “Results from aircraft measurements over White Sands, New Mexico, to calibrate the visible channels of spacecraft instruments,” in *Proc. SPIE*, vol. 924, 1988, pp. 208–214.
- [2] T. N. Carlson and F. E. Boland, “Analysis of urban-rural canopy using a surface heat flux temperature model,” *J. Appl. Meteor.*, vol. 17, pp. 998–1013, 1978.
- [3] T. N. Carlson, “Regional-scale estimates of surface moisture availability and thermal inertia using remote thermal measurements,” *Remote Sensing Rev.* vol. 1, pp. 197–248, 1986.
- [4] T. N. Carlson, J. K. Dodd, S. G. Benjamin, and J. N. Cooper, “Satellite estimation of surface energy balance, moisture availability and thermal inertia,” *J. Appl. Meteor.*, vol. 20, pp. 67–87, 1981.
- [5] T. N. Carlson, E. M. Perry, and T. J. Schmutge, “Remote estimation of soil moisture availability and fractional vegetation cover over patchy vegetation,” *Agricul. Forest Meteorol.*, 1990.
- [6] J. G. Charney, W. J. Quirk, S. H. Chow, and J. Kornfield, “A comparative study of the effects of albedo change on drought in semi-arid regions,” *J. Atmos. Sci.*, vol. 34, pp. 1366–1385, 1977.
- [7] G. Gutman, “The derivation of vegetation indices from AVHRR data,” *Int. J. Remote Sensing*, vol. 8, pp. 1235–1243, 1987.
- [8] ———, “A simple method for estimating monthly mean albedo of land surfaces from AVHRR data,” *J. Appl. Meteor.*, vol. 27, pp. 973–988, 1988.
- [9] B. N. Holben, “Characteristics of maximum value composite images from temporal AVHRR data,” *Int. J. Remote Sensing*, vol. 7, pp. 1417–1434, 1986.
- [10] *Global Vegetation Index User’s Guide*. Washington DC: NOAA, 1986.
- [11] E. Matthews, “Global vegetation and land use: New high-resolution data base for climate studies,” *J. Climate Appl. Meteor.*, vol. 22, pp. 474–587, 1983.
- [12] C. R. Perry and L. R. Lautenschlager, “Functional equivalence of spectral vegetation indices,” *Remote Sensing Environ.*, vol. 14, pp. 169–182, 1984.

- [13] J. C. Price, "On the use of satellite data to infer surface fluxes at meteorological scales," *J. Appl. Meteor.*, vol. 21, pp. 1111-1122, 1982.
- [14] ———, "The potential of remotely sensed thermal infrared data to infer surface soil moisture and evaporation," *Water Resources Res.*, vol. 16, pp. 787-795, 1982.
- [15] ———, "Land surface measurements from the split window channels of the NOAA-7 advanced very high resolution radiometer," *J. Geophys. Res.*, vol. 89, pp. 7231-7237, 1984.
- [16] ———, "Comparison of the information content of data from the Landsat-4 thematic mapper and the multispectral scanner," *IEEE Trans. Geosci. Remote Sensing*, vol. GE-22, pp. 272-281, 1984.
- [17] ———, "Calibration of satellite radiometers and the comparison of vegetation indices," *Remote Sensing Environ.*, vol. 21, pp. 15-27, 1987.
- [18] ———, "An update on visible and near infrared calibration of satellite instruments," *Remote Sensing Environ.*, vol. 24, pp. 419-422, 1988.
- [19] ———, "Erratum, calibration of NOAA 10 AVHRR," *Remote Sensing Environ.*, vol. 26, p. 303, 1988.
- [20] R. R. Nemani and S. W. Running, "Estimation of regional surface resistance to evapotranspiration from NDVI and thermal-IR AVHRR data," *J. Appl. Meteor.*, vol. 28, pp. 276-284, 1989.
- [21] B. Saltzman and J. A. Pollack, "Sensitivity of the diurnal surface temperature range to changes in physical parameters," *J. Appl. Meteor.*, vol. 16, pp. 614-619, 1977.
- [22] M. R. Segal, R. Avissar, M. C. McCumber, and R. A. Pielke, "Evaluation of vegetation effects on the generation and modification of mesoscale circulations," *J. Atmos. Sci.*, vol. 45, pp. 2268-2292, 1988.
- [23] R. J. Sellers, Y. Mintz, Y. C. Sud, and A. Dalcher, "A simple biosphere model (SIB) for use within general circulation models," *J. Atmos. Sci.*, vol. 43, pp. 505-531, 1986.
- [24] O. Taconet, R. Bernard, and D. Vidal-Madjar, "Evapotranspiration over an agricultural region using a surface flux/temperature model based on NOAA-AVHRR data," *J. Climate. Appl. Meteor.*, vol. 25, pp. 284-307, 1986.
- [25] R. M. Teillet *et al.*, "Absolute radiometric calibration of the NOAA advanced very high resolution radiometer (AVHRR) sensors," in *Proc. SPIE*, vol. 924, 1988, pp. 196-207.
- [26] C. J. Tucker, J. R. G. Townsend, and T. E. Goff, "African land-cover classification using satellite data," *Science*, vol. 227, pp. 369-375, 1985.
- [27] C. J. Tucker, "Maximum normalized difference vegetation index images for sub-Saharan Africa for 1983-1985," *Int. J. Remote Sensing*, vol. 7, pp. 1383-1384, 1986.
- [28] C. J. Tucker, "Red and photographic infrared combinations for monitoring vegetation," *Remote Sensing Environ.*, vol. 8, pp. 127-150, 1979.
- [29] *Weekly Weather and Crop Bulletin*, U.S. Dept. Commerce and U.S. Dept. Agriculture, vol. 68, no. 29, pp. 2, 3, 1981.
- [30] P. J. Wetzel, D. Atlas, and R. Woodward, "Determining soil moisture from geosynchronous satellite infrared data: A feasibility study," *J. Climate Appl. Meteor.*, vol. 23, pp. 375-391, 1984.
- [31] H. W. Yates, J. D. Tarpley, S. R. Schnieder, D. F. McGinnis, and R. A. Scofield, "The role of meteorological satellites in agricultural remote sensing," *Remote Sensing Environ.*, vol. 14, pp. 219-233, 1984.

*



John C. Price received the Ph.D degree in physics from the University of California at Berkeley.

He spent 15 years at the NASA/Goddard Space Flight Center, where he developed an interest in the interpretation of satellite data. In 1980 he transferred to the Agricultural Research Service, continuing his studies of analysis methods for inference of evapotranspiration, atmospheric corrections to satellite data, and radiometric calibration.